

# Indium Phosphide MEMS Cantilever Resonator Sensors Utilizing a Pentacene Absorption Layer

Nathan Siwak, Xiao Zhu Fan, Dan Hines, Subramaniam Kanakaraju, Neil Goldsman, and Reza Ghodssi

**Abstract**—We report a microelectromechanical system cantilever waveguide resonator sensing platform utilizing a novel optical readout scheme and the organic semiconductor pentacene as a surface absorbing layer. In this paper, the measurement of isopropyl alcohol and ethanol vapors by way of mass induced frequency shift using a cantilever microbalance is demonstrated. Vapor was introduced to the system through a custom built environmental chamber. A frequency shift due to a mass absorption of 65 Hz was measured, corresponding to a measurement of  $6.92 \pm 1.1 \times 10^{-14}$  g with a minimum detectable mass of  $5.09 \times 10^{-15}$  g for the devices presented. The pentacene absorbing layer in this paper shows it for the first time, functioning as a mass absorbing layer. These results are also the first demonstration of repeatable mass sensing performed using the integrated indium phosphide cantilever waveguide sensor platform. [2008-0134]

**Index Terms**—Chemical sensors, microelectromechanical system (MEMS) cantilevers, pentacene, III–V MEMS.

## I. INTRODUCTION

THE NEED to monitor the environment and detect various chemicals is a critical task for industrial, military, and homeland defense applications. Detecting and identifying chemicals quickly and accurately while requiring low power, and offering high sensitivity, and portability are highly desired for the next generation of chemical sensing technologies. Chemical sensors are constructed from two basic components: a transducer element which converts a mechanical or electrical change in the sensor into a measureable electrical signal and a chemically sensitive and selective layer which serves to bind chemicals to the active area of the transducer element. Both of these components are important in determining the overall performance of the sensor.

There are a number of existing chemical sensors using capacitive, resistive [1], bulk resonance [2], and optical methods [3] to transduce a chemical response into a useable signal.

Manuscript received May 29, 2008; revised August 21, 2008. First published December 12, 2008; current version published February 4, 2009. This work was supported by the National Science Foundation under Grant 0134134. Subject Editor R. T. Howe.

N. Siwak, X. Z. Fan, N. Goldsman, and R. Ghodssi are with the MEMS Sensors and Actuators Laboratory, Department of Electrical and Computer Engineering, Institute for Systems Research, University of Maryland, College Park, MD 20742 USA.

D. Hines is with the Department of Physics, University of Maryland, College Park, MD 20742 USA.

S. Kanakaraju is with The Laboratory for Physical Sciences, College Park, MD 20740 USA.

Color versions of one or more of the figures in this paper are available online at <http://ieeexplore.ieee.org>.

Digital Object Identifier 10.1109/JMEMS.2008.2008600

The performance of these sensors is often limited by large required device sizes, power consumption, and support equipment, which can prevent large-scale integration and portability. For example, surface acoustic wave resonator sensors [2], [4] can be relatively large, making them difficult to integrate into a single-chip array for performing multiple chemical recognition studies. Optical sensors, while often simple, require complex sample preparation and labeling, which reduce the feasibility to use these devices in real-world situations. In addition, readout circuitry can be expensive, power hungry, and more complex than desired for the development of portable sensors.

In contrast to traditional designs, microelectromechanical systems (MEMSs) utilizing mechanical microstructures, such as micromachined cantilevers, provide promising sensor solutions that are small, saleable, low power, and ultimately portable. First demonstrations by Nathanson and Howe [5], [6] using resonant microbridges for filtering and vapor sensing showed the initial promise for these MEMS sensors. Since then, MEMS resonant beam and cantilever sensing has become a well-established method to detect various analytes in an environment. Many of these devices have the advantage of performing detection in a label-free manner [3], [7] and can be mass fabricated in large parallel arrays to perform multiple sensing operations simultaneously. The devices have also proven to be very sensitive. Recent developments have reported detection of the attachment of single cells, DNA, viruses [8], and even attogram-level mass measurements [9].

Traditionally, the most sensitive cantilever sensors have been measured using external optical methods [3], [8], [10], [11]. High displacement resolution allows for lower voltage resonant operation and even the possibility of ambient thermal excitation of resonant cantilevers. The most common measurement technique is similar to that employed in atomic force microscopy (AFM), where a laser is reflected off the cantilever surface onto a position sensitive detector (PSD) [12]. The oscillations of the cantilever can be measured by the continuously changing response of the detector. Other optical methods, such as interferometric measurements [13], can be used to achieve ultrasensitive displacement resolution; however, like AFM techniques, they generally require costly and bulky equipment and infrastructure. Methods, such as piezoelectric [14], piezoresistive [15], and capacitive [16] readout schemes, have also been employed to measure cantilever response; however, they do not offer the same benefits of high displacement sensitivity and relative electrical noise immunity that optical methods exhibit [3].

Chemical sensors use a variety of selective coatings from polymers to self-assembled monolayers (SAMs) [3], [7], [17] to attract chemical species to the active areas of the devices. While these coatings are often highly specific in their response, the vast majority of these coatings are a passive component of the sensor as a whole: A mass absorption or surface stress change is only measured from these layers by the appropriate transducer, and from these effects, the chemical is inferred. To perform the sensing of multiple chemicals in parallel, multiple sensitive layers will be required, which may not be possible in certain situations or may unnecessarily complicate fabrication steps. Active absorption layers have been used in some of the first solid state and current organic chemical field-effect transistor (Chem-FET) sensors [18], [19], which use mobility and charge changes due to the absorption and proximity of chemicals to detect the materials of interest. Ideally, an active absorption layer such as those used in Chem-FETs could be used to measure mechanical effects such as absorption or surface stress and internal electrical changes due to the absorption of analytes simultaneously, reducing the fabrication complexity and maintaining selectivity.

Traditional SAMs are a very common coating to create a functional surface for chemical and biological sensors [3]. The high quality of these films, their ability to be patterned, and their flexibility to be used in a variety of situations have made them a popular choice for chemical coatings. These films are limited to surface sorption effects but can be tailored for very specific chemical or biological attachments.

Polymers such as polyethereurethane, polyimide, or polycarbosilane [20]–[22] are often used as a chemical sensing layer. These layers operate based upon absorption within the polymer to increase mass, volume, or surface stresses, depending on the transducer sensing function desired. These materials are often chosen because of their robustness and ease of use. Many of these polymers can be modified in such a way to increase affinity for various chemicals, but due to various chemical properties (hydrophilicity, polarity, porosity, etc.), they do not always maintain the same type of extremely specific chemical affinities that SAMs provide.

The chemical sensor presented in this paper merges the versatility of MEMS cantilever sensors with the following: 1) an integrated optical readout scheme using end-coupled waveguiding structures first presented by Pruessner *et al.* [23] and, for the first time, 2) an active absorption layer consisting of the organic semiconductor pentacene. Our approach differs from other cantilever sensors in that the measurement of the resonator can be performed using a fully integrated optical readout method. This readout is comparable in displacement sensitivity to the more common AFM-style cantilever measurement and, due to the use of III–V semiconductors, does not require as much external equipment to perform. This provides an advantage for the future integration of these single-chip sensors into portable systems. The use of an active absorption layer pentacene has the potential to increase the selectivity of these chemical sensors by integrating transistor structures within the absorption layer to provide an extra degree of freedom in the chemical sensing measurement provided through the simultaneous electrical and mechanical property interrogation.

## II. PRINCIPLE OF OPERATION

### A. Cantilever Sensing

To perform sensing functions, micromachined cantilevers are coated with specific receptor or absorption coatings. Chemical or biological agents will absorb in this coating, changing the mass of the cantilever and producing a resonant frequency shift [3]. By solving the Euler beam equation for a singly clamped beam and applying this result to Hooke's law, we can determine an expression for the approximate resonant frequency of the structure

$$f_o = \frac{1}{2\pi} \sqrt{\frac{3EI}{L^3 c_o m_o}} \quad (1)$$

where  $E$  is Young's modulus,  $I$  is the cantilever area moment of inertia,  $L$  is the cantilever length,  $m_o$  is the cantilever mass, and  $c_o = 0.24$  is a mass correction factor for a rectangular beam. By separating the mass of the cantilever from the absorbed mass, the shifted frequency due to this additional mass can be shown as

$$f_{\text{shifted}} = \frac{1}{2\pi} \sqrt{\frac{3EI}{L^3 (c_A m_A + c_o m_o)}} \quad (2)$$

where  $m_A$  is the absorbed mass, and  $c_A$  is a constant that describes the position of the added mass ( $0.24 < c_A < 1$ ). Measuring the change in resonant frequency over time exposed to an analyte allows the added mass of the analyte to be calculated using (2). Determining this frequency shift provides information about the specific chemical or biological agents in the environment. This allows the specific analyte mass to be quantitatively measured.

A frequency shift can also be used in a qualitative fashion by detecting a binary response to various chemicals: An appreciable frequency shift indicates the presence of a chemical species, determined by the absorbing material used. A large array of cantilevers with varying absorbing coatings can be fabricated and calibrated to recognize a particular sensor response to analytes of interest [24], [25]. This approach presents itself as a more useful sensing methodology due to its scalability, relative ease of implementation, and ability to screen multiple analytes simultaneously.

### B. Readout Mechanism

The major drawback in using optical readout methods lies in the large free-space optical components (lasers, alignment mirrors, etc.) required, which limit the deployment of these sensors from laboratory use to portable systems. Furthermore, alignment tolerance and accuracy for these methods can be very stringent, as focusing a laser beam onto a microscale device is difficult. Due to these alignment challenges and the necessary reflected optical signals, cantilever device sizes are constrained to designs which allow the beam to be focused onto and reflected from the surface, which can decrease the device sensitivity. To obtain the best displacement resolution, vibration

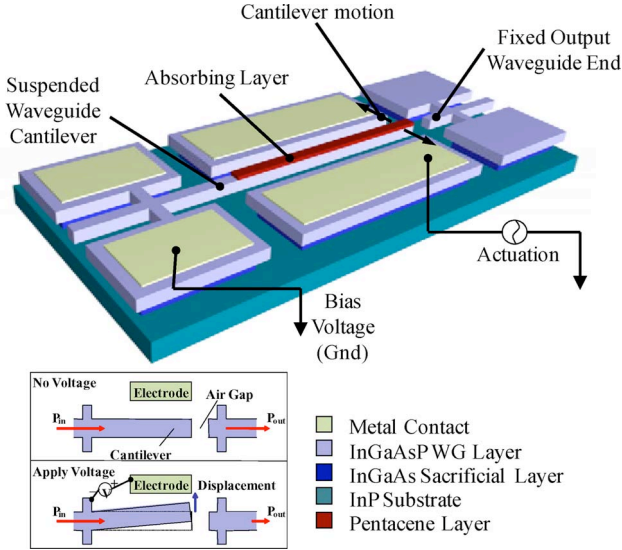


Fig. 1. Cantilever waveguide principle of operation schematic.

isolation, as well as photodetector and sample thermal stability, becomes more critical due to the increased degrees of freedom introduced by the large number of components involved in the measurement setup [26]. The need for noise-free, sensitive, compact, and portable devices, therefore requires a different readout approach.

Our approach to address these issues is a cantilever displacement readout scheme which relies on the change of optical coupling between two waveguides shown schematically in Fig. 1. An input waveguide guides laser light from a lensed fiber through a section of the waveguide that is separated and released from the substrate. As the “free” cantilever waveguide oscillates, it misaligns with a fixed output waveguide, decreasing the optical power coupled to the output waveguide. This output waveguide guides the light to an additional lensed fiber and then to an off-chip photodetector.

This optical coupling due to misalignment provides a very sensitive displacement measurement, with reported displacement resolution comparable to the traditional PSD/reflection readout system ( $\sim 20$  fm/ $\sqrt{\text{Hz}}$ ) [26]. The complexity and amount of external equipment required are reduced significantly using this method, where the alignment procedures for onto and off-chip coupling are simplified. This concept has been used for vibration measurement in harsh environments using a silicon dioxide SiO<sub>2</sub> cantilever waveguide [27] and as a possible replacement for traditional AFM cantilever readouts in force measurements [26].

While sensitive, these reported devices still need external optical sources and often external photodetectors due to the optically passive waveguide structures and indirect bandgap silicon substrates. The III–V direct bandgap semiconductor InP allows for the fabrication of optical sources, photodiodes, and passive waveguide structures within a single substrate by way of molecular beam epitaxy (MBE) growth. Therefore, in the case of using III–V semiconductors, one can fabricate all of the components on-chip monolithically, making single-chip sensors a more viable solution.

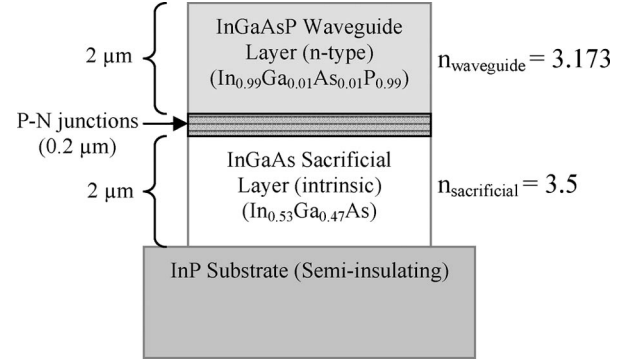


Fig. 2. Layer structure of MBE growth used for cantilever waveguides.

### III. DESIGN

#### A. Cantilever Waveguides

The design of the cantilever waveguides focuses on resonant frequency and constraints of electrostatic actuation, such as the pull-in voltages of the cantilever and the maximum voltages to be applied to the electrodes to perform the actuation. Previous experiments identified a maximum voltage of 26 V, which could be applied to the InP layer structure before breakdown occurs. This limits the stiffness of the cantilever to an extent, as certain pull-in voltages are calculated for a variety of lengths and widths of cantilevers, as well as actuation gaps using the method outlined by [28] and used to determine appropriate actuation gaps and feasible dimensions for the cantilevers. In-plane electrostatic actuation is chosen due to the ability to adjust this actuation air gap and due to an insulating substrate beneath (see Figs. 1 and 2).

The resonant frequency of the cantilever waveguides is used as a design parameter due to its relation to the sensitivity of the device. The mass loading sensitivity can be expressed as [3]

$$\frac{\Delta m}{\Delta f} = \frac{m_o \cdot 0.48}{f_0 c_A} \quad (3)$$

where  $m_o$  is the cantilever mass,  $f_0$  is the resonant frequency, and  $c_A$  is a coefficient from 0.24–1 describing the location of the mass attachment ( $1 =$  concentrated at the cantilever tip). From (3), we see that the sensitivity of the cantilever in question is inversely proportional to the resonant frequency. The resonant frequency of a cantilever can be defined as

$$f_o = \frac{W}{2\pi L^2} \sqrt{\frac{aE}{\rho}} \quad (4)$$

where  $W$  is the cantilever width,  $L$  is the cantilever length (as defined in Fig. 3),  $E$  is the Young’s modulus of InP,  $\rho$  is the density of the cantilever material, and  $a$  is a geometric factor ( $140/132 \approx 1.06$  for a rectangular resection). From (4), we see that increasing the width of the cantilever and decreasing the length of the cantilever will increase its resonant frequency and thus increase the sensitivity of the device, as defined in (3). Higher resonant frequencies exhibit higher quality factors ( $Q$ ), as dampening coefficients decrease with resonator length [29]. Higher  $Q$  factors will lead to more narrow resonance peaks,

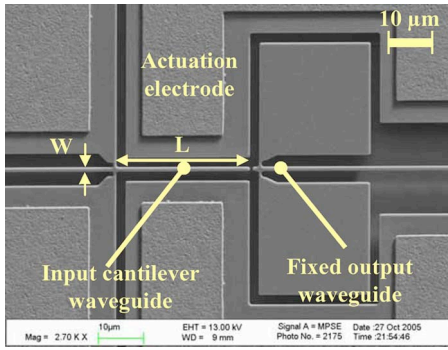


Fig. 3. SEM image of 30- $\mu\text{m}$ -long cantilever showing relevant dimensions.

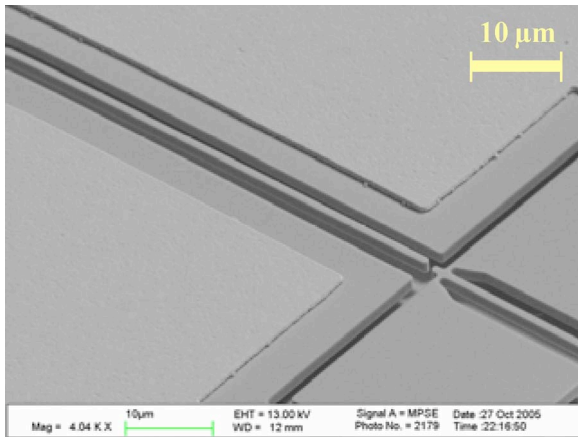


Fig. 4. SEM of the released cantilever waveguide.

thus decreasing the minimum measurable frequency shift ( $\Delta f$ ) which influences the minimum detectable mass.

Ultimate cantilever dimensions are determined by physical and practical limitations. Cantilever width is limited to less than 2  $\mu\text{m}$  to reduce the stiffness of the cantilevers. As the stiffness increases with the width, the displacement of the beam will also decrease to the limit where the displacement is undetectable using reasonable actuation voltages ( $< 26\text{ V}$ ). At wider cantilever dimensions, the sensitivity due to misalignment of the waveguides is also decreased (REF). The length and thickness of the cantilevers are limited by intrinsic stress gradients and MBE growth. An intrinsic arsenic contamination during the MBE growth process creates a static out-of-plane bending of that cantilevers, which is more pronounced at longer device lengths. Devices longer than 100  $\mu\text{m}$  can have nearly 2  $\mu\text{m}$  of out-of-plane bending, fully misaligning the cantilevers and reducing the optical coupling across the gap (for an example of out-of-plane bending, see Fig. 4). MBE growths are limited in thickness due to the agglomeration of defects, and thus, the cantilever thickness has been set at 2  $\mu\text{m}$  to reduce the growth complexity and difficulty.

The Young's modulus (80 GPa) was measured in our previous InP material property studies [30] and used to calculate resonant frequency. Considering them, cantilever waveguide dimensions ranged from 0.6–1.4  $\mu\text{m}$  wide, 10–100  $\mu\text{m}$  long and 2  $\mu\text{m}$  thick. Cantilevers were designed to study a range of resonant frequencies and the limits of our measurement setup.

## B. Absorbing Layer

In any resonant sensor, an interface layer is necessary to absorb or attract a specific chemical species to provide a mechanical change on the device. Various layers are chosen, often based on the type of analyte to be detected or the type of measurement to be used in reading out the sensor. This interface provides selectivity and functionality to an otherwise ordinary resonant mechanical structure.

The organic semiconductor pentacene was chosen as an active absorbing layer for its multimodal sensing potential in both electrical and mechanical domains, as well as compatibility with the cantilever waveguide device fabrication process. Pentacene has been studied over the past few decades as a material for the fabrication of organic semiconductor transistors and circuit elements, as it maintains some of the highest hole mobilities recorded to date. Pentacene and other organic semiconductors have also been used as chemical sensors by measuring the change in mobility due to the interactions with absorbed chemical species. These sensors can suffer from specificity in that many chemicals do not affect the mobility or affect it similarly [18].

While it is most often seen employed as an absorbing layer in solid-state chemical sensors by detecting the charges within the pentacene layer, it has also been reported to absorb vapors and gasses volumetrically in literature [31]. Therefore, pentacene can additionally be used as an absorbing layer for a cantilever microbalance, measuring the molecular weight of an absorbed species. While the microbalance alone may not be very selective between different chemicals, the use of pentacene allows us to increase the potential selectivity by fabricating a solid-state pentacene Chem-FET with the cantilever mass sensor. In this way, it becomes possible to further augment the cantilever microbalance with transistor-based chemical detection in parallel to increase the selectivity of the sensor system in future iterations.

The deposition of materials on existing free-standing structures is also a factor when choosing an absorbing layer for the cantilever sensors. Most polymeric absorbing layers are deposited via solution casting or through spray coating. Due to the release and critical point drying processes employed in the fabrication of our devices, coating the sensors with the materials before undercut and drying is not a viable option, often resulting in the removal of the polymer layers during this process. Coating the cantilever postrelease is also not possible due to stiction phenomena occurring, even for traditional spray coatings which have minimum droplet sizes of up to tens of micrometers. This is incompatible with minimum device feature sizes of 0.6  $\mu\text{m}$ . Pentacene allows for the vapor deposition onto the device structure postrelease without the concerns of stiction. This provides another practical advantage to using this absorbing coating for these devices.

## C. Fabrication

Devices are fabricated from an epitaxially grown substrate using MBE. The layer structure used for our waveguide resonators is shown in Fig. 2. This structure includes P-N junctions

at the InGaAs–waveguide interface to reduce current leakage through the substrate. Very slight mole fractions of gallium and arsenic are introduced in the device layer to create a slight tensile stress to prevent beam buckling.

The two-mask fabrication process flow used is similar to some of our previous work in developing InP suspended waveguides [23], [30], [32], [33]. A silicon dioxide hard mask is deposited (thickness  $\approx 7000$  Å) on a  $15 \times 15$  mm chip and patterned with a  $1\text{-}\mu\text{m}$ -thick resist exposed on a  $5\times$  stepper and a reactive ion etching (RIE) step. A cyclic methane–hydrogen/oxygen plasma RIE is used to etch the InGaAsP and InGaAs layers  $3\text{--}5$   $\mu\text{m}$  deep with better than  $85^\circ$  sidewall angle. Ni–Au–Ge–Ni–Au n-type ohmic contacts are deposited using electron beam evaporation and annealed in a hydrogen atmosphere at  $400$  °C for 40 s. The chip is then thinned to  $150\text{--}200$   $\mu\text{m}$  and cleaved to achieve optical quality waveguide facets. The release of the devices is then performed in a  $\text{HF}:\text{H}_2\text{O}_2:\text{H}_2\text{O}$  (1 : 1 : 8) solution, which etches the InGaAs layer 100% selectively from the waveguide layer. The fabrication process is completed by using a  $\text{CO}_2$  critical point dryer to prevent the cantilevers from experiencing stiction. A released cantilever is shown in Fig. 4.

For this initial experiment where no electronic function is expected, the quality of the organic semiconductor film is not of primary importance as it is with the fabrication of transistors in pentacene [34]. Pentacene films are deposited on a completed and previously characterized cantilever waveguide device using thermal vacuum sublimation, which is a dry deposition method compatible with the current sensor fabrication process. It also minimally affects optical propagation, as its index of refraction is lower than that of InP ( $n_{\text{InP}} \approx 3.1$ ) [35], making it a good match for the cantilever waveguide sensor presented in this paper. Assuming a volumetric absorption, this initial design uses a relatively thick layer (200 nm) to maximize the chemical or vapor absorbed into this coating.

#### IV. TESTING RESULTS

##### A. Cantilever Waveguide Testing Procedures

Device testing was performed by measuring the modulation of light transmitted through the waveguide cantilever while resonating. This was accomplished by coupling light at 1550 nm from a laser source into our devices using a lensed fiber to focus the beam onto the waveguide input facet. A second lensed fiber collects light from the output waveguide facet, which is then measured with a photodetector. The analog photodetector output signal is captured with an oscilloscope and then analyzed using MATLAB. Micropositioner probes are used to make electrical contact to the actuation electrodes to provide in-plane actuation. Actuation of the cantilevers is carried out by applying voltage signals generated with a function generator with approximately 10-V peak-to-peak amplitudes.

The measurement of the resonant frequency was carried out by two techniques: a frequency sweeping and a “tuning fork” ring-down technique. Frequency sweeps were performed by actuating the cantilever waveguides at a known frequency and constant amplitude. The output is measured as a function

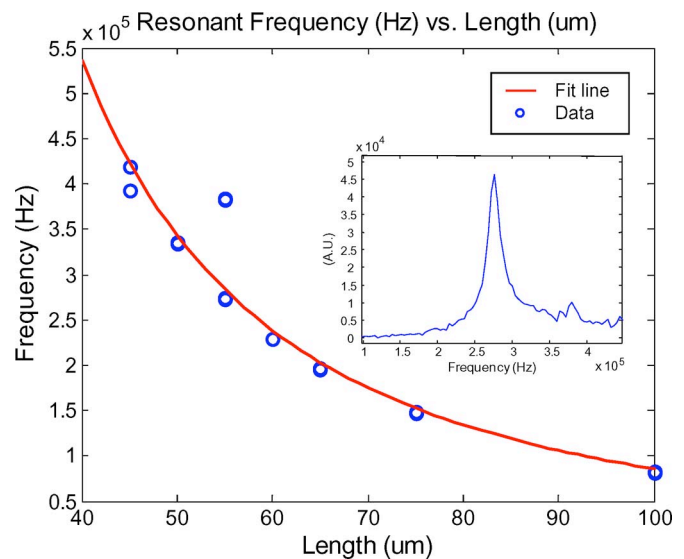


Fig. 5. Plot of the measured resonant frequency versus length. Fit line shows resonant frequency is proportional to  $L^{-2}$  of the cantilever. Cantilevers with length of 45 to 100  $\mu\text{m}$  and a width of 1.2  $\mu\text{m}$  are shown. Inset shows an example of the resonant frequency measurement after Fourier transform of the raw data using the ringing measurement technique.

of the input frequency, where the signal amplitude indicates the relative misalignment of the input cantilever waveguide. This provides a measurement of the motion of the beam. A Lorentzian curve was then fitted to the amplitude versus frequency data to extract the resonant frequency and  $Q$  factor for the cantilever under test. The ringing method employs a dc actuation pulse which actuates the cantilever waveguide to a static displacement and then releases it, allowing it to oscillate to the rest position. This output ringing response takes the form of a decaying sinusoid, which is then analyzed in MATLAB by taking a Fourier transform of the data. To convert the step response into an impulse response, the frequency spectrum obtained by the transform is multiplied by  $j$ . A final Lorentzian fit is made to the frequency spectrum from which resonant frequency and  $Q$  factor are extracted (see inset of Fig. 5).

The frequency sweep technique was first used to analyze uncoated cantilevers due to its ability to analyze devices of all sizes and resonant frequencies. The resonant frequency of the cantilever waveguides ranges from 81.1 kHz ( $W = 1.2$   $\mu\text{m}$ ;  $L = 100$   $\mu\text{m}$ ) to 5.78 MHz ( $W = 0.8$   $\mu\text{m}$ ;  $L = 10$   $\mu\text{m}$ ). As expected, the resonant frequency of the cantilever is inversely proportional to  $L^2$  of the cantilever, as shown in Fig. 5. The 5.78-MHz resonant frequency cantilever with a quality factor of 356 ( $W = 0.8$   $\mu\text{m}$ ;  $L = 10$   $\mu\text{m}$ ) has the highest frequency and quality factor that have been obtained using the current testing setup, which is an improvement over past reported results [36]. The  $Q$  factor is expected to be directly proportional to the resonant frequency [37], [38] with the general trend agreeing, as shown in Fig. 6. The drawback of the frequency sweep technique is the time required to perform the measurement, which is the primary reason why it was abandoned in later tests.

The ringing measurement method was chosen for all environmental tests for its relatively fast data acquisition ( $\sim 1$  s) and ease of direct implementation into the data acquisition and analysis setup. Due to breakdown voltages, the sizes of

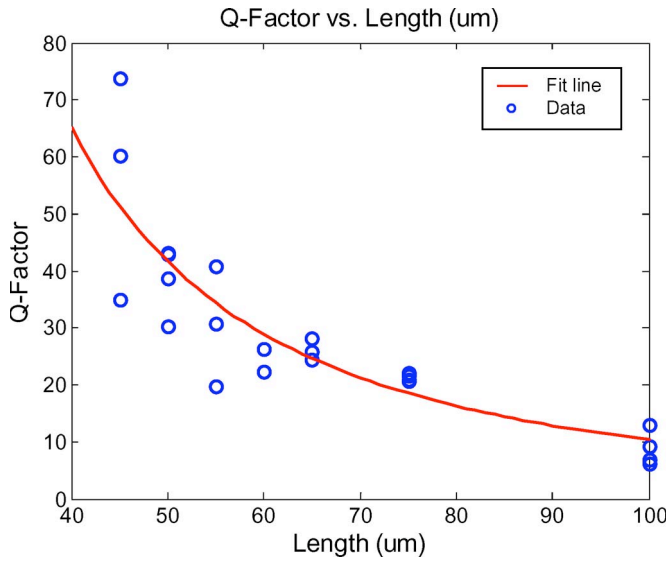


Fig. 6. Plot of calculated quality factor versus length. The general trend of  $Q$  factor is proportional to  $L^{-2}$  of the cantilever and, thus, directly proportional to resonant frequency. Cantilevers with length of 45 to 100  $\mu\text{m}$  and a width of 1.2  $\mu\text{m}$  are shown.

testable cantilevers were limited to medium lengths, rather than the high-frequency devices. With increased stiffness of shorter cantilevers, dc actuation becomes more difficult without implementing a gated sinusoidal actuation scheme to more efficiently resonate the cantilevers. This gated sinusoidal actuation signal can create inconsistencies in measurements due to a frequency tuning effect caused by a required dc voltage offset in the signal and therefore is currently not being used for actuation. To balance the actuation voltage limits and the resulting resonant frequency, cantilevers with 60- $\mu\text{m}$  length were chosen for this initial mass sensing experiment.

Testing cantilever waveguides with the pentacene layer required initial characterization of the device and a chemical sensor setup that required a controlled environment. The same characterization techniques used for the standard cantilever waveguides, frequency sweep, and ring down were applied to cantilever waveguides with a deposited pentacene layer. The increase in mass due to the deposition of pentacene resulted in a negative frequency shift of 1.61 kHz, corresponding to a mass increase of 9.701 pg. With a known deposition thickness of pentacene of 200 nm on a known cantilever ( $W = 1.2 \mu\text{m}$ ;  $L = 60 \mu\text{m}$ ), the density of the deposited pentacene was calculated to be 673.7  $\text{kg}/\text{m}^3$ , which is in relatively good agreement with bulk phase density of  $\approx 1000 \text{ kg}/\text{m}^3$  [39]. No measurable difference in the  $Q$  factor was seen after the pentacene deposition.

The chemical sensor setup requires the delivery of the analyte to the cantilever's pentacene coated surface. Isopropyl alcohol [(IPA); 60.10 g/mol] and ethanol vapor (46.07 g/mol) were chosen due to their high vapor pressure at room temperature, nonreactive nature with air, nontoxicity, availability, and ease of use. The fluid was stored in a bubbler (300-mL glass filtering flask with internal tubing) attached to a dispensing system which consisted of a plastic capillary and rubber tubing. An inert carrier gas, nitrogen ( $\text{N}_2 = 28.0 \text{ g}/\text{mol}$ ), was introduced into the bubbler and transported the vapors to the device surround-

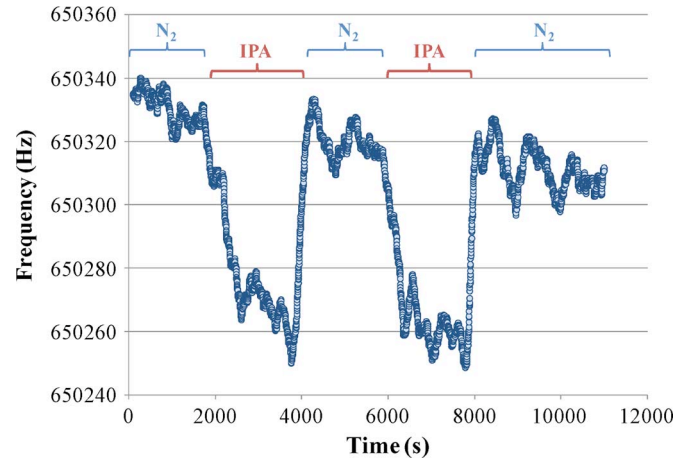


Fig. 7. Frequency versus time under exposure to IPA for two exposure cycles, showing a consistent frequency shift of approximately  $-65 \text{ Hz}$  in the resonant frequency. The long term drift is attributed to changes in ambient conditions and actuator drift.

ings. Temperature and humidity were also monitored during the testing of chemical sensors. The estimated concentrations of IPA and ethanol vapors were 58 000 ppm, and 61 000 ppm, respectively.

Testing was performed by first purging the environmental chamber with  $\text{N}_2$ , establishing a baseline measurement of the resonant frequency. IPA vapors were then introduced to the system along with the  $\text{N}_2$  carrier gas. Each vapor introduction cycle consisted of 33 min of exposure to the gas mixture, with ring-down resonant frequency collection every 2 s. After this exposure, the flow through the bubbler was again switched to a pure  $\text{N}_2$  flow to recover the system and desorb the vapors. This process was repeated a number of times for both IPA and ethanol vapors.

## V. RESULTS AND DISCUSSION

The resonant frequency of the cantilever waveguide with a pentacene layer was tracked to detect the mass change due to the introduction of IPA and ethanol vapors. The fitted resonant frequency versus time, shown in Fig. 7 for IPA vapors and Fig. 8 for ethanol, shows an average resonant frequency shift of  $-65.0 \text{ Hz}$  for both cases. This shift in resonant frequency corresponds to a mass increase of  $6.92 \pm 1.1 \times 10^{-14} \text{ g}$ . An exponential decay function was fitted to the trend of the data, with an estimated time constant of the absorption to be about 5.3 min for IPA vapors and 4.2 min for ethanol vapor. In both cases, full recovery to the original baseline resonant frequency was obtained after purging with  $\text{N}_2$ .

A drift was experienced over the data range, which can be attributed to optical fiber misalignment due to electrostrictive actuator drift and the change in environmental conditions over the duration of the day of the measurement (morning to night). The actuator movement did not affect the absolute frequency shift experienced by the resonators but did increase the uncertainty of the measurements. In one instance, the misalignment caused a loss in resonant frequency peaks, shown by the region of missing data in Fig. 8. Both the IPA and ethanol caused statistically identical frequency shifts, which may be a result

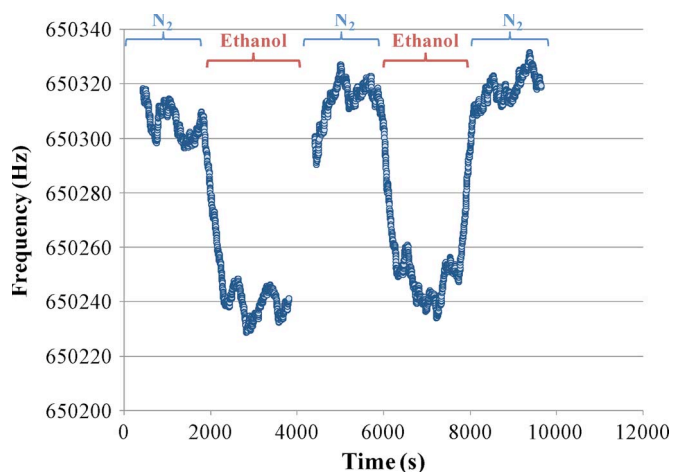


Fig. 8. Frequency versus time under exposure to ethanol for two exposure cycles, showing the same consistent frequency shift of  $-65$  Hz in resonant frequency. The long term drift is attributed to changes in ambient conditions and actuator drift. Note the missing data at 4000 s, which can be attributed to the significant misalignment of input and output optical fibers.

of the molecule size compared to the available volume for absorption within the pentacene layer. It is possible that a chemical reaction between ambient environment and IPA such as the oxidation of pentacene to pentacenequinone [31] may have contributed to the change in the absorption properties of the film during the first absorption measurements, making the two vapors indistinguishable. In addition, the time constants of the absorption of IPA and ethanol are not drastically different from one another. Response time seems to show a slight decrease with smaller molecules (ethanol), which may indicate the absorption mechanism is related to molecule size. The temperature differences of the vapors between the absorption and desorption may have affected the relative rates of diffusion into and out of the pentacene layer. More detailed investigation of the pentacene absorbing layer is required to fully explain these phenomena.

For this initial experiment, the large pentacene film thickness was deposited based upon incomplete previous knowledge of this film's sorptive behavior. A thinner layer would change the absorption parameters, possibly speeding up the process. Thinner layers also produce higher quality film growths and would be more suited for the fabrication of organic transistors within the layer [40]. Further optimization of the pentacene layer thickness will assist not only in understanding the absorption mechanisms but also improving the response time and selectivity of the sensor [21].

Based upon the mass sensitivity calculated from (3) by estimating a minimum  $\Delta f$  from the standard deviation of baseline measurements, we can measure a minimum  $\Delta m$  of  $5.09 \times 10^{-15}$  g using these devices. We believe that this minimum  $\Delta m$  is largely limited by the current testing setup and can be further decreased by reducing the noise due to the inline photodetector, transmission line effects due to external cabling, and ambient mechanical vibration, actuator drift, and air currents affecting the placement of lensed fibers and, thus, the optical coupling into and out of the waveguide facets. The removal of just one lensed fiber from the optical setup by integrating an on-chip photodiode will reduce noise due to ambient

vibrations and actuator drift. The next step toward single-chip sensor technology requires the introduction of on-chip monolithic photodetectors and sources, which will greatly enhance the sensitivity of the cantilever waveguide sensors by reducing on- and off-chip coupling losses due to waveguide-fiber mode mismatch, misalignment, and vibration.

Future design work will concentrate on increasing the cantilever  $Q$  factor, as discussed previously, to facilitate a lower minimum  $\Delta m$ , since this will directly affect the performance of the device in the improved next generation testing setup. For these cantilever waveguides tested, the  $Q$  factor in air was calculated to be  $\sim 60$  due to high viscous and squeeze film damping losses. As an example of future possibilities, cantilevers with a length of  $10 \mu\text{m}$  have been characterized in the megahertz range of resonant frequencies with  $Q$  factors surpassing 300 in air. Assuming similar noise sources and levels, this would equate to a minimum  $\Delta m$  of  $5.0 \times 10^{-16}$  g, which is possible with this high-frequency cantilever. Along with the improvement of the testing setup, such as the introduction of a lock-in amplifier and/or a feedback loop to inflate the  $Q$  factor, these devices would further increase the mass sensitivity of our system due to the increased intrinsic  $Q$  factor arising from decreased dampening losses at higher operating frequencies. High-frequency cantilever waveguides are currently undergoing more thorough testing and characterization before environmental testing.

## VI. CONCLUSION

A resonant cantilever sensor with a novel optical readout has been successfully designed, fabricated, and tested. The chemical sensor utilizes an InP cantilever waveguide resonator coated with a pentacene thin film absorption layer. A resonant frequency shift is measured due to the volumetric absorption of IPA and ethanol into the deposited thin film pentacene. Unlike conventional cantilever piezoelectric or capacitive readout, this system takes advantage of the high resolution and sensitivity of an optical readout, which utilizes the cantilever as a resonator, as well as an optical waveguide. Improvement in selectivity of the chemical sensor can be further investigated with the integration of pentacene solid-state sensors, which will require additional tailoring of the pentacene layer. The measurements of various explosive vapors and other harmful organic vapors can also be carried out to more clearly establish the selectivity of the pentacene absorbing layer in the context of the cantilever sensors. Using these cantilever waveguide resonators, the minimum measurable  $\Delta m$  is  $2.23 \times 10^{-15}$  g. However, higher sensitivity can be obtained by utilizing cantilevers with higher resonant frequency and  $Q$  factor. Further efforts to improve the testing setup by decreasing electrical and photodetector noise will increase the potential sensitivity as well.

This paper represents the first significant step toward the use of InP in a chemical sensing system. Future work will take full advantage of the III-V materials being used in the fabrication of our cantilever waveguides to demonstrate the integration of on-chip optical sources and photodetectors to decrease the testing setup complexity. The design and implementation of an on-cantilever pentacene Chem-FET device will be one of the first demonstrations of an active absorbing layer being utilized on a

cantilever transducer and will be the final step toward the development of selective, sensitive, and compact single-chip sensors.

#### ACKNOWLEDGMENT

The authors would like to thank the Laboratory for the Physical Sciences cleanroom staff for the assistance with the device fabrication and J. McGee for the helpful discussions on data analysis.

#### REFERENCES

- [1] E. S. Snow, F. K. Perkins, E. J. Houser, S. C. Badescu, and T. L. Reinecke, "Chemical detection with a single-walled carbon nanotube capacitor," *Science*, vol. 307, no. 5717, pp. 1942–1945, Mar. 2005.
- [2] M. C. Horrillo, J. Lozano *et al.*, "Wine classification with a zinc oxide SAW sensor array," *Sens. Actuators B, Chem.*, vol. 120, no. 1, pp. 166–171, Dec. 2006.
- [3] N. V. Lavrik, M. J. Sepaniak, and P. G. Datskos, "Cantilever transducers as a platform for chemical and biological sensors," *Rev. Sci. Instrum.*, vol. 75, no. 7, pp. 2229–2253, Jul. 2004.
- [4] S. J. Ippolito, A. Ponzoni, K. Kalantar-Zadeh, W. Wlodarski, E. Comini, G. Faglia, and G. Sberveglieri, "Layered  $\text{WO}_3/\text{ZnO}/36^\circ\text{LiTaO}_3$  SAW gas sensor sensitive towards ethanol vapour and humidity," *Sens. Actuators B, Chem.*, vol. 117, no. 2, pp. 442–450, Oct. 2006.
- [5] H. C. Nathanson, W. E. Newell, R. A. Wickstrom, and J. R. Davis, Jr., "The resonant gate transistor," *IEEE Trans. Electron Devices*, vol. ED-14, no. 3, pp. 117–133, Mar. 1967.
- [6] R. T. Howe and R. S. Muller, "Resonant-microbridge vapor sensor," *IEEE Trans. Electron Devices*, vol. ED-33, no. 4, pp. 499–506, Apr. 1986.
- [7] R. Berger, C. Gerber, H. P. Lang, and J. K. Gimzewski, "Micromechanics: A toolbox for femtoscale science: 'Towards a laboratory on a tip,'" *Microelectron. Eng.*, vol. 35, no. 1–4, pp. 373–379, Mar. 1997.
- [8] B. Ilic, D. Czaplowski, M. Zalalutdinov, H. G. Craighead, P. Neuzil, C. Campagnolo, and C. Batt, "Single cell detection with micromechanical oscillators," *J. Vac. Sci. Technol.*, vol. B19, no. 6, pp. 2825–2828, Nov. 2001.
- [9] B. Ilic, H. G. Craighead, S. Krylov, W. Senaratne, and C. Ober, "Atto-gram detection using nanoelectromechanical oscillators," *J. Appl. Phys.*, vol. 95, no. 7, pp. 3694–3703, Apr. 2004.
- [10] S. Dohn, R. Sandberg, W. Svendsen, and A. Boisen, "Enhanced functionality of cantilever based mass sensors using higher modes and functionalized particles," in *Proc. 13th Int. Conf. Solid-State Sens., Actuators, Microsyst. (Transducers)*, Seoul, South Korea, 2005, pp. 636–639.
- [11] N. V. Lavrik and P. G. Datskos, "Femtogram mass detection using photothermally actuated nanomechanical resonators," *Appl. Phys. Lett.*, vol. 82, no. 16, pp. 2697–2699, Apr. 2003.
- [12] L. A. Pinnaduwa, V. Boiadjev, J. E. Hawk, and T. Thundat, "Sensitive detection of plastic explosives with self-assembled monolayer-coated microcantilevers," *Appl. Phys. Lett.*, vol. 83, no. 7, pp. 1471–1473, Aug. 2003.
- [13] B. Ilic, S. Krylov, K. Aubin, R. Reichenbach, and H. G. Craighead, "Optical excitation of nanoelectromechanical oscillators," *Appl. Phys. Lett.*, vol. 86, no. 19, pp. 193 114–193 114-3, May 2005.
- [14] Y. Lee, G. Lim, and W. Moon, "A self-excited micro cantilever biosensor actuated by PZT using the mass micro balancing technique," *Sens. Actuators A, Phys.*, vol. 130/131, pp. 105–110, Aug. 2006.
- [15] P. Li and X. Li, "A single-sided micromachined piezoresistive  $\text{SiO}_2$  cantilever sensor for ultra-sensitive detection of gaseous chemicals," *J. Micromech. Microeng.*, vol. 16, no. 12, pp. 2539–2546, Dec. 2006.
- [16] E. Forsen, G. Abadal *et al.*, "Ultrasensitive mass sensor fully integrated with complementary metal-oxide-semiconductor circuitry," *Appl. Phys. Lett.*, vol. 87, no. 4, pp. 043 507-1–043 507-3, Jul. 2005.
- [17] M. F. Mabrook, C. Pearson, and M. C. Petty, "Inkjet-printed polymer films for the detection of organic vapors," *IEEE Sensors J.*, vol. 6, no. 6, pp. 1435–1444, Dec. 2006.
- [18] B. Crone, A. Dodabalapur, A. Gelperin, L. Torsi, H. E. Katz, A. J. Lovinger, and Z. Bao, "Electronic sensing of vapors with organic transistors," *Appl. Phys. Lett.*, vol. 78, no. 15, pp. 2229–2231, Apr. 2001.
- [19] J. N. Zemel, "Ion sensitive field effect transistors and related devices," *Anal. Chem.*, vol. 47, no. 2, p. 255A, 258-9, 264-5, 268, 1975.
- [20] Y.-H. Kim, K. Jang, Y. J. Yoon, and Y.-J. Kim, "A novel relative humidity sensor based on microwave resonators and a customized polymeric film," *Sens. Actuators B, Chem.*, vol. 117, no. 2, pp. 315–322, Oct. 2006.
- [21] F. Lochon, L. Fadel, I. Dufour, D. Rebière, and J. Pistré, "Silicon made resonant microcantilever—Dependence of the chemical sensing performances on the sensitive coating thickness," *Mater. Sci. Eng. C*, vol. 26, pp. 348–353, 2006.
- [22] I. Voiculescu, M. E. Zaghoul, R. A. McGill, E. J. Houser, and G. K. Fedder, "Electrostatically actuated resonant microcantilever beam in CMOS technology for the detection of chemical weapons," *IEEE Sensors J.*, vol. 5, no. 4, pp. 641–647, Aug. 2005.
- [23] M. W. Pruessner, K. Amarnath, M. Datta, D. Kelly, S. Kanakaraju, P.-T. Ho, and R. Ghodssi, "InP-based optical waveguide MEMS switches with evanescent coupling mechanism," *J. Microelectromech. Syst.*, vol. 14, no. 5, pp. 1070–1081, Oct. 2005.
- [24] S.-H. Lim, D. Raorane, S. Satyanarayana, and A. Majumdar, "Nanochemo-mechanical sensor array platform for high-throughput chemical analysis," *Sens. Actuators B, Chem.*, vol. 119, no. 2, pp. 466–474, Dec. 2006.
- [25] D. Then, A. Vidic, and C. Ziegler, "A highly sensitive self-oscillating cantilever array for the quantitative and qualitative analysis of organic vapor mixtures," *Sens. Actuators B, Chem.*, vol. 117, no. 1, pp. 1–9, Sep. 2006.
- [26] K. Zinoviev, C. Dominguez, J. A. Plaza, V. J. C. Busto, and L. M. Lechuga, "A novel optical waveguide microcantilever sensor for the detection of nanomechanical forces," *J. Lightw. Technol.*, vol. 24, no. 5, pp. 2132–2138, May 2006.
- [27] E. Ollier, P. Philippe, C. Chabrol, and P. Mottier, "Micro-opto-mechanical vibration sensor integrated on silicon," *J. Lightw. Technol.*, vol. 17, no. 1, pp. 26–29, Jan. 1999.
- [28] S. Pamidighantam, "Pull-in voltage analysis of electrostatically actuated beam structures with fixed-fixed and fixed-free end conditions," *J. Micromech. Microeng.*, vol. 12, no. 4, pp. 458–464, Jul. 2002.
- [29] H. Hosaka, K. Itao, and S. Kuroda, "Damping characteristics of beam-shaped micro-oscillators," *Sens. Actuators A, Phys.*, vol. 49, no. 1/2, pp. 87–95, Jun. 1995.
- [30] M. W. Pruessner, T. King, D. Kelly, R. Grover, L. C. Calhoun, and R. Ghodssi, "Mechanical property measurement of InP-based MEMS for optical communications," *Sens. Actuators A, Phys.*, vol. 105, no. 2, pp. 190–200, Jul. 2003.
- [31] O. D. Jurchescu, J. Baas, and T. T. M. Palstra, "Electronic transport properties of pentacene single crystals upon exposure to air," *Appl. Phys. Lett.*, vol. 87, no. 5, pp. 052 102-1–052 102-3, Aug. 2005.
- [32] M. Datta, M. W. Pruessner, K. Amarnath, J. McGee, S. Kanakaraju, and R. Ghodssi, "Wavelength-selective integrated optical MEMS filter in InP," in *Proc. 18th Int. Conf. Micro Electro Mech. Syst.*, Miami Beach, FL, 2005, pp. 88–91.
- [33] M. W. Pruessner, M. Datta, K. Amarnath, S. Kanakaraju, and R. Ghodssi, "Indium phosphide based MEMS end-coupled optical waveguide switches," in *Proc. 17th Int. Indium Phosphide Related Mater. Conf.*, Glasgow, U.K., 2005, pp. 110–113.
- [34] S. R. Forrest, "Ultrathin organic films grown by organic molecular beam deposition and related techniques," *Chem. Rev.*, vol. 97, no. 6, pp. 1793–1896, Oct. 1997.
- [35] S. P. Park, S. S. Kim, J. H. Kim, C. N. Whang, and S. Im, "Optical and luminescence characteristics of thermally evaporated pentacene films on Si," *Appl. Phys. Lett.*, vol. 80, no. 16, pp. 2872–2874, Apr. 2002.
- [36] M. W. Pruessner, N. Siwak, K. Amarnath, S. Kanakaraju, W.-H. Chuang, and R. Ghodssi, "End-coupled optical waveguide MEMS devices in the indium phosphide material system," *J. Micromech. Microeng. (JMM)*, vol. 16, no. 4, pp. 832–842, Apr. 2006.
- [37] M. Alvarez, J. Tamayo, J. A. Plaza, K. Zinoviev, C. Dominguez, and L. M. Lechuga, "Dimension dependence of the thermomechanical noise of microcantilevers," *J. Appl. Phys.*, vol. 99, no. 2, pp. 024 910-1–024 910-7, Jan. 2006.
- [38] J.-H. Lee, S.-T. Lee, C.-M. Yao, and W. Fang, "Comments on the size effect on the microcantilever quality factor in free air space," *J. Micromech. Microeng.*, vol. 17, no. 1, pp. 139–146, Jan. 2007.
- [39] I. Yagi, K. Tsukagoshi, and Y. Aoyagi, "Growth control of pentacene films on  $\text{SiO}_2/\text{Si}$  substrates towards formation of flat conduction layers," *Thin Solid Films*, vol. 467, no. 1/2, pp. 168–171, Nov. 2004.
- [40] M. M. Ling and Z. Bao, "Thin film deposition, patterning, and printing in organic thin film transistors," *Chem. Mater.*, vol. 16, no. 23, pp. 4824–4840, 2004.

Authors' photographs and biographies not available at the time of publication.